第 43 卷 第 14 期/2023 年 7 月/光学学报 研究论文

光学学报

基于远场同轴全息的激光 M^2 因子测量技术

李俊博[1,2]，刘斯靓[1,2]，韩志刚[1,2*]，李方欣[1,2]，杨振营[1,2]，芮九多[1,2]，王琦[1,2]，朱日宏[1,2]

[1]南京理工大学电子工程与光电技术学院，江苏 南京 210094；

[2]南京理工大学先进固体激光工信部重点实验室，江苏 南京 210094

摘要 激光光束质量 M^2 因子的动态测量对激光器的设计、制造与应用均具有重要意义。本文提出了一种基于远场同轴全息的光纤激光器光束质量 M^2 因子动态测量方法。通过偏振移相同轴全息技术直接获取待测激光的远场复振幅信息，利用角谱传输及透镜变换理论求解激光在自由空间中的光场强度分布，从而实现 M^2 因子的动态测量。实验搭建了远场同轴全息装置，测量了不同纤芯直径光纤在 632.8 nm 波长下的激光光束质量，其结果与 BEAM SQUARED 商用光束质量仪的测量结果一致。本文所提方法仅需 0.02 s 即可实现光纤激光的 M^2 因子测量，比商用光束质量仪的测量速度提高了两个数量级以上。此外，本装置结构紧凑，能够避免透镜引入的装调及加工误差。

关键词 光纤光学与光通信；光束质量 M^2 因子；同轴移相干涉；角谱传输；透镜变换

中图分类号 O436 **文献标志码** A **DOI**：10.3788/AOS230593

1 引 言

光纤激光器以光纤作为激光的传输介质，具有结构紧凑、转化效率高、能实现能量柔性传输等特点，在工业、国防等领域得到了广泛的应用[1-5]。光束质量是光纤激光器的核心参数之一，直接决定激光的作用与传播效果[6]。目前已有多种光束质量参数被提出，如光束质量 M^2 因子[7]、斯特列尔比[8]、桶中功率[9]和衍射极限倍数[10]等，其中光束质量 M^2 因子只与待测激光有关，并且可以同时反映出激光的近场和远场分布，是一种相对较为完善的激光光束质量评价参数[11]。随着激光功率的提升，激光器中热积累和非线性效应会引起光束质量的动态变化[12]。动态获取光纤激光的光束质量有利于揭示激光器模场动态变化的物理机制，控制和利用激光模场分布，对激光器的设计、制造与应用均具有极为重要的意义。

多点拟合法是目前公认的一种光束质量测量方法[13]，其通过采集聚焦激光束腰附近不同位置的光斑强度分布，然后利用双曲线方程拟合确定光束的束腰大小与远场发散角，进而获取激光光束质量 M^2 因子。该方法虽然简单，但需要引入准直和聚焦透镜实现光束聚焦，在光束质量测量中引入了透镜的装调和加工误差。此外，受限于测量速度，该方法无法实现光束质量的动态测量。

为实现光束质量 M^2 因子的快速测量，多种方法被相继提出。基于变焦距思想的液体透镜法[14-16]和空间光调制器法[17-18]可实现时间低于 1 s 的 M^2 因子测量，但在实际应用中易受温度、重力等环境影响和低分辨率的限制。法布里-珀罗（F-P）腔法[19]和衍射光栅法[20]仅需单个 CCD 即可实时测量出激光在不同位置的光斑大小，但是该类方法由于系统参数和结构相对固定，对激光束的准直具有较高的要求。散射光成像法[21]利用成像系统对聚焦后的强激光所散射出的光成像来获取激光的传播轨迹，从而达到测量 M^2 因子的目的，该方法适合于测量强激光的光束质量，但其精度易受环境影响。

复振幅重构法是实现光束质量实时测量的一种有效方法。该方法通过复原出待测激光的复振幅信息，然后结合标量衍射理论将复原出的复振幅进行虚拟传输与分析，进而计算出待测激光的光束质量 M^2 因子。该方法主要分为两类：数值分析法[22-24]和波前测量法[25-27]。基于数值分析的光束质量测量方法需要首先测量输出光束的近场和远场光强分布，然后通过数值算法使得重构的光强分布与实测的光强分布相同。最典型的有 G-S 算法[28]，该方法结构简单、鲁棒性高，对实验仪器要求不高，但收敛速度较慢。光强传输方程（TIE）[29]也是一种通过重构激光复振幅测算 M^2 因子的常用算法。该算法无需迭代，单次 M^2 因子测量时间为 0.5 s 左右，但是在测量模式复杂的光纤激光时，存在复振幅重构和 M^2 因子测量不准确的问题。波前

收稿日期：2023-02-24；**修回日期**：2023-03-17；**录用日期**：2023-03-24；**网络首发日期**：2023-05-08

基金项目：国家自然科学基金（61875087）

通信作者：*hannjust@163.com

测量法采用波前传感器直接测量得到激光复振幅。2001年，Neal等[30]提出了使用哈特曼波前传感器来动态测量M^2因子，但分辨率较低，难以应用到实际测量。此后，Du等[31]和Han等[32]分别基于离轴全息和四波横向剪切干涉技术实现了光束质量M^2因子的动态测量。由于存在频谱欠采样等问题[33]，这两种方法恢复复杂模场相位的精度还有待分析。

本文提出了一种基于远场同轴全息的光纤激光光束质量M^2因子动态测量方法。该方法基于偏振移相的同轴全息系统获取4幅同轴全息干涉图，然后通过移相法动态解调待测激光复振幅信息，再结合虚拟传输获取激光近场附近多个位置的光强分布，最终计算得到待测激光的M^2因子。该方法采用远场同轴全息技术，无需复杂光学系统即可获取激光近场信息。相比于离轴全息技术，本文所提方法在不引入离轴像差的前提下，能够快速、高精度、高分辨率地获取复振幅信息，实现了激光光束质量M^2因子的快速准确测量。

2　基本原理

基于远场同轴全息的光束质量测量系统光路如图1所示。待测激光经过分光棱镜(BS)分成两路，BS透射光的P分量透过偏振合束棱镜(PBC)作为测试光，BS的反射光耦合至单模光纤形成单模激光输出。由于PBS透射P光反射S光的特性，参考光的S分量和测试光的P分量合束后透射经过1/4波片(QWP)，然后被分别调整成左旋和右旋圆偏振光并由偏振探测器接收。偏振探测器是由像素化的微透镜阵列、微偏振阵列以及面阵探测器构成，微偏振像元的透光轴方位角共有四种，分别为0°、45°、90°、135°。因此，左旋圆偏振参考光以及右旋圆偏振光测试光在偏振探测器上能同步形成携带待测光波前信息的4幅移相干涉图[34]，其强度分布可表示为

$$I_k(x,y)=A(x,y)+C(x,y)\cos\varphi\left[(x,y)+k\frac{\pi}{2}\right],\quad(1)$$

式中：$A(x,y)=I_r(x,y)+I_t(x,y)$为干涉图背景，$I_r(x,y)$、$I_t(x,y)$分别为参考光和测试光的强度分布；$C(x,y)=2\sqrt{I_r(x,y)\cdot I_t(x,y)}$为干涉图对比度；$\varphi(x,y)$为测试光相对于参考光的相位分布；$k$依次为0、1、2、3，代表不同的偏振方向。

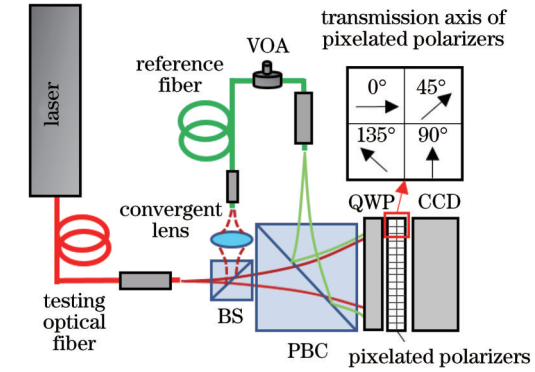

BS: beam splitter; PBC: polarization beam combiner;
VOA: variable optical amplifier; QWP: quarter wave plate;
CCD: charge coupled device

图1　基于远场同轴全息的光束质量M^2因子测量系统光路

Fig. 1　Optical path of beam quality factor M^2 measurement system based on far-field coaxial holography

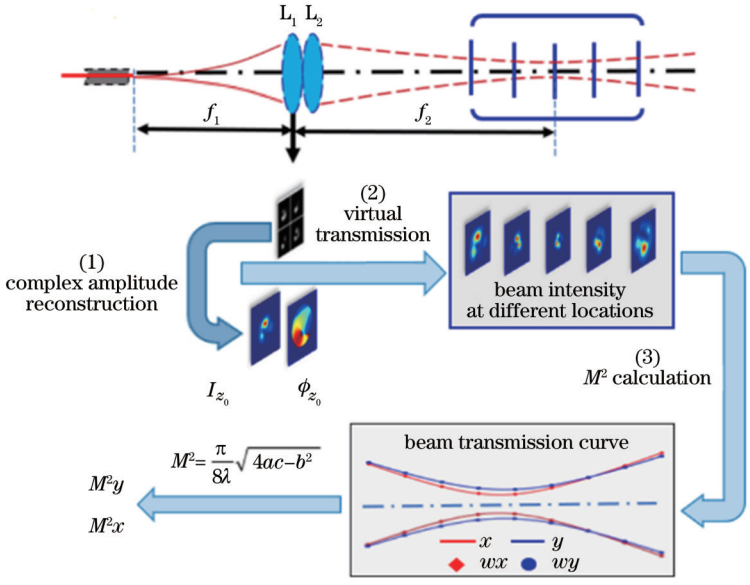

图2　光束质量M^2因子计算流程

Fig. 2　Calculation process of beam quality factor M^2

图2为基于远场复振幅的光束质量的计算流程，包括三个步骤：1)复振幅恢复；2)虚拟传输；3)光束质量M^2因子计算。首先通过干涉图的同步移相解调得到测试光的相位分布$\varphi(x,y)$及其强度分布$I(x,y)$。

在相机靶面位置设置焦距为f_1的虚拟透镜L_1，f_1为光纤端面距离偏振相机靶面的等效光程，测试光经L_1准直后的复振幅分布可表示为

$$E_0(x,y)=\sqrt{I(x,y)}\exp\left[\mathrm{i}\varphi(x,y)\right]。\tag{2}$$

根据ISO 11146标准，计算M^2因子需获得束腰附近不同位置的光强分布，直接将准直光的复振幅$E_0(x,y)$作基于快速傅里叶变换（FFT）的角谱传输可能会遇到频率传递函数欠采样等问题。因此，本文在虚拟透镜L_1相同位置还设置了焦距为f_2的虚拟透镜L_2，经过L_2后准直光变成了会聚光，如图2所示。L_2后焦面附近不同位置的光场分布可表示为

$$E_i(x,y)=\mathscr{F}^{-1}\left\{\mathscr{F}\left[E_0(x,y)\exp\left(-\mathrm{i}\pi\frac{x^2+y^2}{\lambda f_2}\right)\right]H(f_x,f_y,z_i)\right\},\tag{3}$$

式中：z_i表示E_i所在平面与L_2后表面的距离；f_x、f_y表示光场的频域坐标；$H(f_x,f_y,z_i)$为复振幅在自由空间的频域传递函数。距离透镜L_2后表面z_i处的光强分布表示为$I_i(x,y)=\left|E_i(x,y)\right|^2$。采用光强二阶矩算法计算不同位置光斑的束宽$d_i$，$d_i$与$z_i$满足双曲线关系$d_i^2=a+bz_i+cz_i^2$。利用莱文贝格-马夸特（Levenberg-Marquardt，L-M）方法[35]即可拟合出式（3）中的系数，即可计算出激光的光束质量M^2因子：

$$M^2=\frac{\pi}{8\lambda}\sqrt{4ac-b^2}。\tag{4}$$

3　实验装置

远场同轴全息实验装置如图3所示。实验采用中心波长为633 nm的光纤耦合单频半导体激光器（PL-NL-633，LD-PD INC，Singapore）作为系统光源。输出激光由分光比为50∶50的1×2光纤分束器（630-HP光纤，MC light，China）分成两路，其中一路光纤的输出光S分量经边长为10 mm的PBC（Jinda Optics，China）反射后作为参考光，另一路光纤熔接不同型号的测试光纤，其输出光的P分量透过PBC作为测试光。测试光纤分别为Nufern 630 HP，Nufern 1060 XP以及Corning SMF-28e。参测光经过1/4波片（4级，Jinda Optics，China）后产生同轴全息图，由偏振相机（PHX050S，Lucid）采集4幅移相干涉图。该同轴全息系统十分紧凑，尺寸约为50 mm×30 mm×30 mm。偏振相机拍摄的全息图由个人计算机（联想Y7000P，CPU：i7-10875H，RAM：16 GB）分析，最终计算得到不同测试光纤输出激光的光束质量M^2因子。

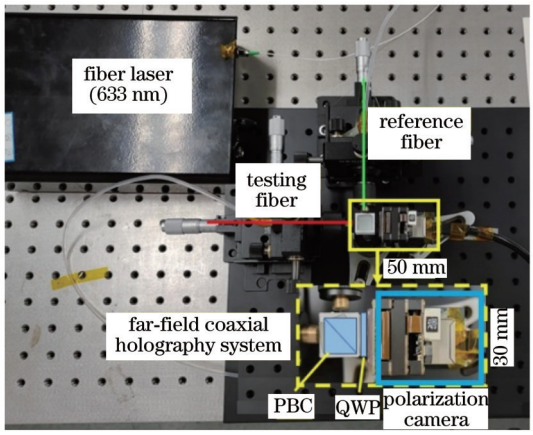

图3　远场同轴全息实验装置

Fig. 3　Experimental setup of far-field coaxial holography

4　结果与讨论

图4（a）为采用SMF-28e作为待测光纤时偏振相

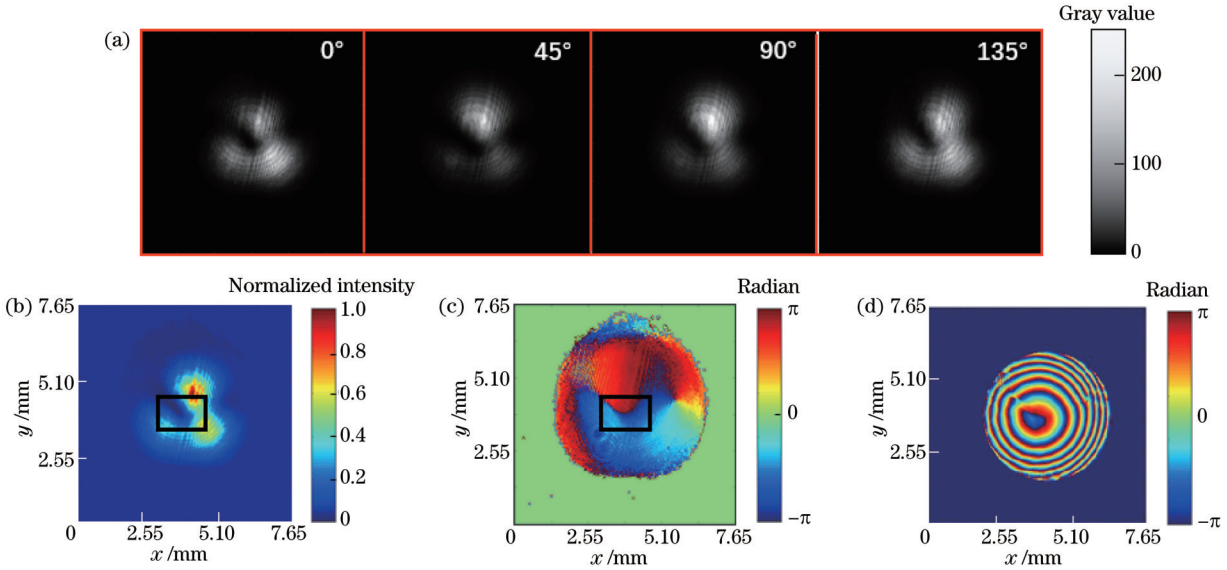

图4　干涉图及复振幅恢复结果。（a）偏振相机采集的单次曝光干涉图；（b）复原光强；（c）复原相位；（d）透镜L_2后表面相位分布

Fig. 4　Interferograms and recovered complex amplitude. (a) Single-shot interferograms taken by polarization camera; (b) recovered intensity; (c) recovered phase; (d) phase distribution at rear surface of lens L_2

机采集的一组干涉图，干涉图对应的偏振方向分别为0°、45°、90°和135°，相邻干涉图具有90°的移相间隔。干涉图尺寸为7.65 mm×7.65 mm，像素个数为300 pixel×300 pixel。图4(b)和4(c)分别是干涉图经四步移相算法解调得到的光强和相位分布，由图中黑框内的区域可以看出，本文所示波前重构方法对弱光强处的阶跃相位信息也能呈现较好的结果。图4(d)为4(b)、4(c)所示复振幅传输到透镜L_2后表面的相位分布。经过透镜后，测试光的相位分布由近似平面转变为会聚球面。

将虚拟透镜L_2后表面的复振幅进行进一步的虚拟传输可以得到其焦点附近各个位置的光强分布。由于透镜后表面为会聚光束，传输过程中不存在角谱传输过程的欠采样问题。采用二阶矩算法计算各位置激光的束宽，最后通过L-M算法对激光束宽和传播距离进行了双曲线拟合，进而计算出激光光束质量M^2因子，其曲线拟合结果及M^2因子结果如图5所示。计算得到的x和y方向上的M^2因子分别为1.794和2.251。除此之外，还可以从拟合曲线上得到其他光束的轮廓信息，如x和y方向上的束腰位置(590.31 mm，587.32 mm)，束腰半径(0.160 mm，0.166 mm)和瑞利距离(70.73 mm，61.01 mm)。

图6表示了不同M^2因子测量过程的时间随图像尺寸的变化。当干涉图尺寸从50 pixel×50 pixel变为500 pixel×500 pixel时，所需时间从0.015 s增加到0.200 s。图6还给出了M^2因子测量结果随图像尺寸的变化。当干涉图尺寸大于80 pixel×80 pixel时，x和y方向上的M^2因子分别约为1.8和2.2。当图像尺寸为50 pixel×50 pixel时，两方向上的M^2因子分别约为2.3和6.0，与干涉图尺寸大于80 pixel×80 pixel的M^2因子测量结果存在较大偏差。100 pixel×100 pixel的干涉图足以对传输10个线偏振(LP)模式的光纤激光进行M^2因子测量，时间仅为0.02 s。

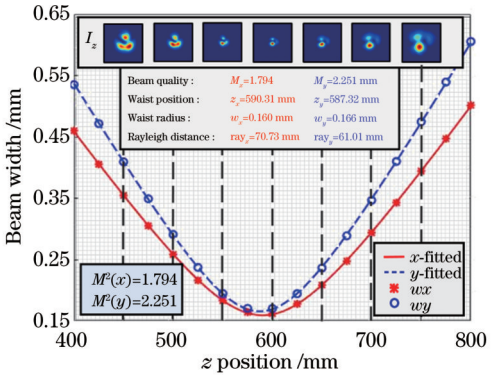

图5　曲线拟合及M^2因子计算结果

Fig. 5　Curve fitting and calculation results of factor M^2

为了验证本文光束质量M^2因子测量方法的准确性，在相同环境下搭建了基于商用光束质量仪BEAM SQUARED的M^2因子测量系统，如图7虚线框内装置所示。该系统通过无限远共轭的显微物镜使光纤输出激光准直，然后通过两个镀铝反射镜将激光反射到BEAM SQUARED光束质量测量仪中，并使激光束光轴与光束测量仪光轴重合。相比于虚线框内系统，本文提出的同轴全息光束质量测量系统(实线框内)的结构更加紧凑。需要说明的是，为了保证两套测量系统的一致性，虚线框内系统仅测量P光的光束质量。

本文采用两套系统分别对型号为630-HP(Nufern)、1060-XP(Nufern)和SMF-28e(Corning)的测试光纤进行了光束质量M^2因子测量，当激光器输出波长为632.8 nm时，这三种光纤在单一偏振方向上能传输的模式数目分别为1、6和10。图8为这3种光纤在其固定姿态下的测量结果。以三次结果的均值作为M^2因子测量结果。图中还对比了两种方法束腰位置的光强分布。对于630-HP光纤，本文所提方法的测量结果为$M^2_{x_c}=1.09$，$M^2_{y\_c}=1.03$，BEAM SQUARED光束质量仪的测量结果为$M^2_{x_m}=1.04$，

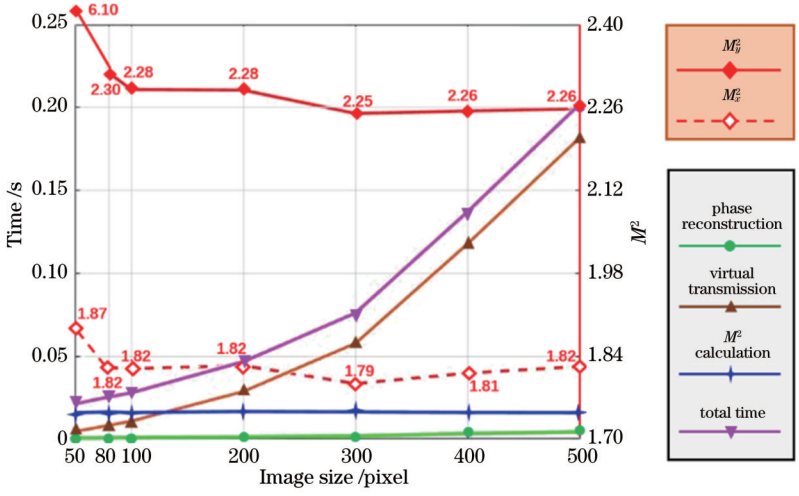

图6　光束质量测量过程随图像尺寸变化的时间特性

Fig. 6　Time characteristic of beam quality measurement process varying with image size

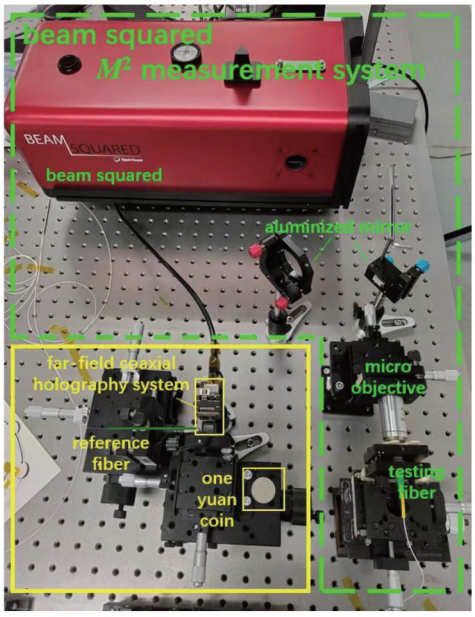

图 7　精度验证实验装置

Fig. 7　Experimental setup for precision verification

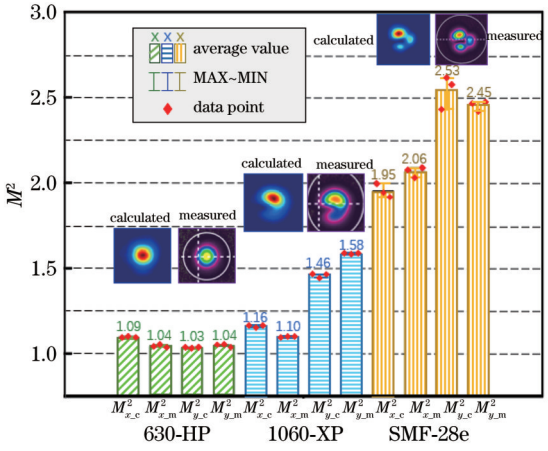

图 8　三种测试光纤的 M^2 因子测量结果

Fig. 8　Measurement results of factor M^2 for three different testing fibers

$M^2_{y\_m}$=1.04。M^2 因子测量平均误差为 0.028。对于 1060-XP 光纤，本文所提方法的测量结果为 $M^2_{x\_c}$=1.16，$M^2_{y\_c}$=1.46，BEAM SQUARED 光束质量仪的测量结果为 $M^2_{x\_m}$=1.10，$M^2_{y\_m}$=1.58。M^2 因子测量平均误差为 0.065。对于 SMF-28e 光纤，本文所提方法的测量结果为 $M^2_{x\_c}$=1.95，$M^2_{y\_c}$=2.53，BEAM SQUARED 光束质量仪的测量结果为 $M^2_{x\_m}$=2.06，$M^2_{y\_m}$=2.45。M^2 因子测量平均误差为 0.043。光束质量验证实验中，为避免反复搭建测量装置引入系统误差，采取将待测光纤分别接入两测量系统的方式进行对比分析。但是在切换测量系统时，光纤姿态会有微小的改变，这会改变激光的输出模场从而造成待测光 M^2 因子的测量误差。该误差在模式数目较多时较为明显，过多的模式数目会导致模式耦合，这也是上述实验结果中 SMF-28e 多次测量的重复性较差的原因。

5　结　　论

本文提出了一种基于同轴全息的光纤激光光束质量 M^2 因子的动态测量方法。该方法基于偏振移相点衍射系统同步获取 4 幅同轴全息干涉图，通过四步移相法及虚拟传输技术获取激光近场附近多个位置的光强分布，最后通过多点拟合法求出待测激光的光束质量 M^2 因子。实验搭建了远场同轴全息的光束质量测量系统，对不同种类的光纤进行了 M^2 因子测量实验，并与商用光束质量分析仪的测量结果进行了对比分析，其结果具有较好的一致性。该方法仅需单次曝光即可实现一次 M^2 因子测量，且单次测量时间最短可达 0.02 s。另外，无镜成像系统的采用使得其实验装置简单紧凑且易于调整，可在不引入离轴像差及透镜像差的前提下实现快速、高精度、高分辨率的复振幅信息获取，进而可实现快速准确的激光光束质量 M^2 因子测量。该方法为光纤激光器的实时质量检测及状态监控提供了技术手段。

参　考　文　献

[1] 虞钢，虞和济. 集成化激光智能加工工程[M]. 北京：冶金工业出版社，2002.
Yu G, Yu H J. Integrated laser intelligent manufacturing[M]. Beijing: Metallurgical Industry Press, 2002.

[2] 陈建华，郑也，刘小溪，等. 高功率激光合束的指向控制分析及研究进展[J]. 导航与控制，2022，21(2)：8-20.
Chen J H, Zheng Y, Liu X X, et al. Analysis and research progress on pointing control of high power laser beam combination[J]. Navigation and Control, 2022, 21(2): 8-20.

[3] 杨保来，杨欢，王鹏，等. 基于自研光纤的 LD 泵浦光纤激光器实现 10 kW 输出[J]. 中国激光，2022，49(20)：2016001.
Yang B L, Yang H, Wang P, et al. LD pumped fiber laser based on self-developed fiber realizes 10 kW output[J]. Chinese Journal of Lasers, 2022, 49(20): 2016001.

[4] 肖虎，潘志勇，陈子伦，等. 基于自研光纤和器件实现 20 kW 高光束质量激光稳定输出[J]. 中国激光，2022，49(16)：1616002.
Xiao H, Pan Z Y, Chen Z L, et al. Stable output of 20 kW high beam quality laser based on self-developed optical fiber and device[J]. Chinese Journal of Lasers, 2022, 49(16): 1616002.

[5] 吴函烁，李瑞显，肖虎，等. 双向级联泵浦部分掺杂光纤实现近 8 kW 高光束质量激光输出[J]. 中国激光，2022，49(7)：0716002.
Wu H S, Li R X, Xiao H, et al. Two-way cascade pumping partially doped fiber to achieve high beam quality laser output of nearly 8 kW[J]. Chinese Journal of Lasers, 2022, 49(7): 0716002.

[6] 牛燕雄，汪岳峰，刘新，等. 激光束质量因子 M^2 及其测量[J]. 激光技术，1999，23(1)：38-41.
Niu Y X, Wang Y F, Liu X, et al. Laser beam quality factor M^2 and its measurement[J]. Laser Technology, 1999, 23(1): 38-41.

[7] Siegman A E. New developments in laser resonators[J]. Proceedings of SPIE, 1990, 1224: 2-14.

[8] Mahajan V N. Strehl ratio for primary aberrations: some analytical results for circular and annular pupils[J]. Journal of the Optical Society of America A, 1982, 72(9): 1258-1266.

[9] 谈斌，杨晓燕. 卡式系统装调对高功率激光光束远场聚焦性能影响研究[J]. 光学与光电技术，2021，19(5)：61-66.

Tan B, Yang X Y. Study on the influence of alignment of cassegrain system on the propagation properties and beam control of high-power lasers[J]. Optics & Optoelectronic Technology, 2021, 19(5): 61-66.

[10] Siegman A E. Analysis of laser beam quality degradation caused by quartic phase aberrations[J]. Applied Optics, 1993, 32(30): 5893-5901.

[11] 孟令强. 基于四波横向剪切干涉的高功率光纤激光光束质量测量技术研究[D]. 南京: 南京理工大学, 2020: 2-5.
Meng L Q. Research on high-power fiber laser beam quality measurement technology based on four-wave transverse shear interference[D]. Nanjing: Nanjing University of Science and Technology, 2020: 2-5.

[12] 陶汝茂. 高功率窄线宽近衍射极限光纤激光放大器热致模式不稳定研究[D]. 长沙: 国防科学技术大学, 2015.
Tao R M. Study of thermal-induced modal instabilities in high power narrow-linewidth fiber amplifiers with near diffraction-limited beam quality[D]. Changsha: National University of Defense Technology, 2015.

[13] ISO. Laser and laser-related equipment: test methods for laser beam widths, divergence angles and beam propagation ratios: ISO-11146[S]. Geneve: International Organization for Standardization, 2021.

[14] Sheikh M, Riza N A. Motion-free hybrid design laser beam propagation analyzer using a digital micromirror device and a variable focus liquid lens[J]. Applied Optics, 2010, 49(16): D6-D11.

[15] Niederriter R D, Gopinath J T, Siemens M E. Measurement of the M^2 beam propagation factor using a focus-tunable liquid lens [J]. Applied Optics, 2013, 52(8): 1591-1598.

[16] Ji K H, Hou T R, Li J B, et al. Fast measurement of the laser beam quality factor based on phase retrieval with a liquid lens[J]. Applied Optics, 2019, 58(11): 2765-2772.

[17] Efron U. Spatial light modulator technology: materials, devices, and applications[M]. New York: Marcel Dekker, 1995.

[18] Schulze C, Flamm D, Duparré M, et al. Beam-quality measurements using a spatial light modulator[J]. Optics Letters, 2012, 37(22): 4687-4689.

[19] Scaggs M, Haas G. Real time laser beam analysis system for high power lasers[J]. Proceedings of SPIE, 2011, 7913: 791306.

[20] Cortés R, Villagómez R, Coello V, et al. Laser beam quality factor (M2) measured by distorted Fresnel zone plates[J]. Revista Mexicana De Física, 2008, 54(4): 279-283.

[21] Jorge K C, Riva R, Rodrigues N A S, et al. Scattered light imaging method (SLIM) for characterization of arbitrary laser beam intensity profiles[J]. Applied Optics, 2014, 53(20): 4555-4564.

[22] Huang L J, Guo S F, Leng J Y, et al. Real-time mode decomposition for few-mode fiber based on numerical method[J]. Optics Express, 2015, 23(4): 4620-4629.

[23] An Y, Huang L J, Li J, et al. Learning to decompose the modes in few-mode fibers with deep convolutional neural network[J]. Optics Express, 2019, 27(7): 10127-10137.

[24] Manuylovich E S, Dvoyrin V V, Turitsyn S K. Fast mode decomposition in few-mode fibers[J]. Nature Communications, 2020, 11(1): 1-9.

[25] Paurisse M, Lévèque L, Hanna M, et al. Complete measurement of fiber modal content by wavefront analysis[J]. Optics Express, 2012, 20(4): 4074-4084.

[26] Lyu M, Lin Z Q, Li G W, et al. Fast modal decomposition for optical fibers using digital holography[J]. Scientific Reports, 2017, 7(1): 1-9.

[27] Li J B, Zhang X Y, Zheng Y H, et al. Fast fiber mode decomposition with a lensless fiber-point-diffraction interferometer[J]. Optics Letters, 2021, 46(10): 2501-2504.

[28] Gerchberg R. A practical algorithm for the determination of phase from image and diffraction plane pictures[J]. Optik, 1972, 35: 237-246.

[29] Teague M R. Deterministic phase retrieval: a Green's function solution[J]. Journal of the Optical Society of America A, 1983, 73(11): 1434-1441.

[30] Neal D R, Gruetzner J K, Roller J P. Use of beam parameters in optical component testing[J]. Proceedings of SPIE, 2001, 4451: 394-405.

[31] Du Y Z, Fu Y Q, Zheng L X. Complex amplitude reconstruction for dynamic beam quality M^2 factor measurement with self-referencing interferometer wavefront sensor[J]. Applied Optics, 2016, 55(36): 10180-10186.

[32] Han Z G, Meng L Q, Huang Z Q, et al. Determination of the laser beam quality factor (M^2) by stitching quadriwave lateral shearing interferograms with different exposures[J]. Applied Optics, 2017, 56(27): 7596-7603.

[33] Zhao W L, Wei C L, Yuan C J, et al. A flexible numerical calculation method of angular spectrum based on matrix product [J]. Optics Letters, 2020, 45(21): 5937-5940.

[34] 郑东晖. 空间相移干涉测量方法及其关键技术研究[D]. 南京: 南京理工大学, 2019: 17-19.
Zheng D H. Research on spatial phase-shifting interferometry and its key technologies[D]. Nanjing: Nanjing University of Science and Technology, 2019: 17-19.

[35] Ahearn T S, Staff R T, Redpath T W, et al. The use of the Levenberg-Marquardt curve-fitting algorithm in pharmacokinetic modelling of DCE-MRI data[J]. Physics in Medicine and Biology, 2005, 50(9): N85-N92.

Measurement Technology of Laser M^2 Factor Based on Far-Field Coaxial Holography

Li Junbo[1,2], Liu Siliang[1,2], Han Zhigang[1,2*], Li Fangxin[1,2], Yang Zhenying[1,2], Rui Jiuduo[1,2], Wang Qi[1,2], Zhu Rihong[1,2]

[1]*College of Electronic Engineering and Optoelectronic Technology, Nanjing University of Science and Technology, Nanjing* 210094, *Jiangsu, China*;

[2]*MIIT Key Laboratory of Advanced Solid Laser, Nanjing University of Science and Technology, Nanjing* 210094, *Jiangsu, China*

Abstract

Objective Fiber lasers have been widely used in industry, national defense, and other fields, with the advantages of compact structure, high efficiency, and flexible energy transmission. Beam quality is one of the most important parameters of the fiber laser and directly determines the performance and propagation effects of the laser. Various beam quality parameters have been proposed so far, such as factor M^2, Strehl ratio, barrel power, and diffraction limit multiples. In all these parameters, factor M^2 is a relatively perfect evaluation parameter of the laser beam quality and can reflect both the near-field and far-field characteristics of the laser. With the increase in the laser power, thermal accumulation and nonlinear effects in the laser can cause dynamic changes in the beam quality. Dynamic measurement of factor M^2 is beneficial to reveal the physical mechanism of mode field changes of the laser and control the real-time distribution of the laser mode field. Therefore, it has great significance to the design, manufacture, and application of lasers.

Methods In this study, we propose a dynamic measurement method of factor M^2 of a fiber laser using coaxial interferometry. The far-field complex amplitude of the laser under test is determined by the spatially phase-shifted coaxial interferograms. The intensity distributions of the laser at different places in the vicinity of the laser near-field are then obtained through angular spectrum transmission and lens transformation. Factor M^2 of the laser is finally determined by fitting the beam diameters at different places. Our new method has a compact structure that avoids manufacturing and assembly errors caused by optical lenses. Compared with off-axis holographic technology, the method described in this study can obtain fast, high-precision, and complex amplitude information with high resolution and realize the fast and accurate measurement of laser beam quality factor M^2 factor.

Results and Discussions In order to verify the feasibility of the factor M^2 measurement method, the measured results of lasers from different fibers are compared with those measured by the commercial factor M^2 measurement system (BEAM SQUARED). Two experimental setups are shown in Fig. 7. The fiber laser under test is collimated by an infinitely conjugated microscope objective lens and then reflected into the commercial factor M^2 measurement system through two aluminized mirrors, as shown in the dashed box of Fig. 7. Through comparison, our coaxial interferometer in the solid line frame of the figure is more compact. It should be noted that to ensure the consistency of the laser under test in the two measurement systems, we only measure the beam quality of the P-light in the dashed box.

Figure 8 shows the factor M^2 results of the output from 630-HP fiber (Nufern), 1060-XP fiber (Nufern), and SMF-28e fiber (Corning) with two different systems shown in Fig. 7. The three fibers can transmit 1, 6, and 10 modes in a single polarization direction, respectively. For each fiber laser, we repeat the measurement three times and use their average values as the results. Figure 7 also compares the light intensity at the waist position with different methods. For 630-HP fiber, the measurement result of the proposed method is $M^2_{x\_c}=1.09$ and $M^2_{y\_c}=1.03$, and that of the commercial BEAM SQUARED is $M^2_{x\_m}=1.04$ and $M^2_{y\_m}=1.04$. The average measurement error of M^2 is 0.028. For 1060-XP fiber, the measurement result of the proposed method is $M^2_{x\_c}=1.16$ and $M^2_{y\_c}=1.46$, and that of the commercial BEAM SQUARED is $M^2_{x\_m}=1.10$ and $M^2_{y\_m}=1.58$. The average measurement error of M^2 is 0.065. For SMF-28e fiber, the measurement result of the proposed method is $M^2_{x\_c}=1.95$ and $M^2_{y\_c}=2.53$, and that of the commercial BEAM SQUARED is $M^2_{x\_m}=2.06$ and $M^2_{y\_m}=2.45$. The average measurement error of M^2 is 0.043. In the verification experiment of the beam quality, in order to avoid the system error introduced by building the measurement system repeatedly, we only move the fiber to be tested to switch the system. However, when the measurement system is switched, the attitude of the optical fiber will be slightly changed, which will change the output mode field of the laser and thus cause the measurement error of M^2 of the beam to be measured. The error is more obvious when the number of modes is large, and excessive modes will lead to mode coupling, which is also the reason for the poor repeatability of multiple

measurements of SMF-28e in the above experimental results.

Conclusions We propose a new method for the dynamic measurement of beam quality factor M^2 of a fiber laser by using far-field coaxial interferometry. The far-field complex amplitude of the laser under test is determined by the spatially phase-shifted coaxial interferograms. The intensity distributions of the laser at different places of free space are then obtained through angular spectrum transmission and lens transformation. factor M^2 of the laser is finally determined by fitting the beam diameters at different places. In the experiment, we have measured factor M^2 of the laser output from fibers with different core diameters at 633 nm. The results are consistent with those determined by the commercial beam quality instrument. In addition, it takes 0.02 s to complete the factor M^2 calculation of lasers by the proposed method, which is more than two orders of magnitude faster than that of the commercial instrument. Our new method has a compact structure that avoids manufacturing and assembly errors caused by optical lenses. The method provides a technical means for the quality detection and state monitoring of few-mode fibers and their devices and is conducive to the design, manufacture, and development of fiber lasers and their fiber devices.

Key words fiber optics and optical communications; beam quality factor M^2; phase-shifted coaxial interference; angular spectrum transmission; lens transformation